# Supporting Information

## Ambient Electrosynthesis of Ammonia Using Core-Shell Structured Au@C Catalyst Fabricated by One-Step Laser-Ablation Technique

Wenyi Li,[a,b†] Chao Zhang,[a,b†] Miaomiao Han,[a] Yixing Ye,[a] Shengbo Zhang,[a,b] Yanyan Liu,[a,b] Guozhong Wang,[a] Changhao Liang,[a,*] and Haimin Zhang [a,*]

[a] Key Laboratory of Materials Physics, Centre for Environmental and Energy Nanomaterials, Anhui Key Laboratory of Nanomaterials and Nanotechnology, CAS Center for Excellence in Nanoscience, Institute of Solid State Physics, Chinese Academy of Sciences, Hefei 230031 Anhui, PR China

[b] University of Science and Technology of China, Hefei 230026, China

[*] Corresponding Authors.

E-mail address: zhanghm@issp.ac.cn. chliang@issp.ac.cn.

[†] These authors contributed equally to this work.

**Table S1.** The comparison of our work and other recently reported NRR electrocatalysts.

| Catalyst | System /Conditions | $NH_3$ Yield Rate | $NH_3$ Yield Rate ($\mu g\ h^{-1}\ cm^{-2}$) | FE (%) | Detection method | Ref. |
|---|---|---|---|---|---|---|
| Au@C | 0.1 M $Na_2SO_4$ (pH=6.3) | 241.9 $\mu g\ h^{-1}\ mg_{cat.}^{-1}$ (-0.45 V *vs.* RHE) | 38.7 $\mu g\ h^{-1}\ cm^{-2}$ (-0.45 V *vs.* RHE) | 40.5 | Indophenol method | This work |
| Au /$TiO_2$ | 0.1 M HCl | 21.4 $\mu g\ h^{-1}\ mg_{cat.}^{-1}$ (-0.2 V *vs.* RHE) | 21.4 $\mu g\ h^{-1}\ cm^{-2}$ (-0.2 V vs. RHE) | 8.11 | Indophenol method | 1 |
| Au nanorods | 0.1 M KOH | 1.648 $\mu g\ h^{-1}\ cm^{-2}$ (-0.2 V *vs.* RHE) | 1.648 $\mu g\ h^{-1}\ cm^{-2}$ (-0.2 V *vs.* RHE) | 3.87 | Nesslers method | 2 |
| Au/CeOx-RGO | 0.1 M HCl | 8.3 $\mu g\ h^{-1}\ mg_{cat.}^{-1}$ (-0.2 V *vs.* RHE) | 1.66 $\mu g\ h^{-1}\ cm^{-2}$ (-0.2 V vs. RHE) | 10.10 | Nesslers method | 3 |
| Au/C | 0.1 M KOH | 0.3 $\mu g\ mg_{metal}^{-1}\ h^{-1}$ (-0.05 V *vs.* RHE) | 0.09 $\mu g\ h^{-1}\ cm^{-2}$ (-0.05 V vs. RHE) | 1.2 | Indophenol method | 4 |
| Au film | 0.1 M KOH | $3.84 \times 10^{-12}$ mol $cm^{-2}\ s^{-1}$ (-0.5 V *vs.* RHE) | 0.235 $\mu g\ h^{-1}\ cm^{-2}$ (-0.5 V vs. RHE) | 0.12 | Indophenol method | 5 |
| NCM-Au | 0.1M HCl (pH =1) | 0.36 g $m^{-2}\ h^{-1}$ (-0.2 V *vs.* RHE) | 36 $\mu g\ h^{-1}\ cm^{-2}$ (-0.2 V vs. RHE) | 22 (-0.1 V *vs.* RHE) | Indophenol method | 6 |
| Au flowers | 0.1 M HCl | 25.57 $\mu g\ h^{-1} mg_{cat.}^{-1}$ (-0.2 V *vs.* RHE) | 15.34 $\mu g\ h^{-1}\ cm^{-2}$ (-0.2 V vs. RHE) | 6.05 | Indophenol method | 7 |
| Au nanocages | 0.5 M $LiClO_4$ | 3.9 $\mu g\ cm^{-2}\ h^{-1}$ (-0.5 V *vs.* RHE) | 3.9 $\mu g\ h^{-1}\ cm^{-2}$ (-0.5 V vs. RHE) | 30.2 (-0.4 V *vs.* RHE) | Nesslers method | 8 |
| Au nanocages | 0.5 M $LiClO_4$ | 3.74 $\mu g\ cm^{-2}\ h^{-1}$ (-0.4 V *vs.* RHE) | 3.74 $\mu g\ h^{-1}\ cm^{-2}$ (-0.4 V vs. RHE) | 35.9 | Nesslers method | 9 |
| AuSAs-NDPCs | 0.1 M HCl | 2.32 $\mu g\ cm^{-2}\ h^{-1}$ (-0.3 V *vs.* RHE) | 2.32 $\mu g\ h^{-1}\ cm^{-2}$ (-0.3 V vs. RHE) | 12.3 | Indophenol method | 10 |
| Ag-Au@ZIF | $LiCF_3SO_3$ 1% EtOH in THF | 10 pmol $cm^{-2}\ s^{-1}$ (-2.9 V vs. Ag/AgCl) | 0.612 $\mu g\ h^{-1}\ cm^{-2}$ (-2.9 V vs. Ag/AgCl) | 18±4 | Indophenol method | 11 |
| $Au_1/C_3N_4$ | 0.005 M $H_2SO_4$ | 1,305 $\mu g\ h^{-1}\ mg_{Au}^{-1}$ (-0.1 V vs. RHE) | 1.74 $\mu g\ h^{-1}\ cm^{-2}$ (-0.1 V vs. RHE) | 11.1 | Indophenol method | 12 |
| pAu/NF | 0.1 M $Na_2SO_4$ | 9.42 $\mu g\ h^{-1}\ cm^{-2}$ (-0.2 V vs. NHE) | 9.42 $\mu g\ h^{-1}\ cm^{-2}$ (-0.2 V vs. RHE) | 26.99 (-0.1 V *vs.* RHE) | Indophenol method | 13 |
| Au@$CeO_2$ | 0.01 M $H_2SO_4$ | 28.2 $\mu g\ h^{-1}\ cm^{-2}$ (-0.4 V vs. RHE) | 28.2 $\mu g\ h^{-1}\ cm^{-2}$ (-0.4 V vs. RHE) | 9.5 | Indophenol method | 14 |
| Au/$Ti_3C_2$ | 0.1 M HCl | 30.06 $\mu g\ h^{-1}\ mg^{-1}$ 4(-0.2 V *vs.* RHE) | 76.68 $\mu g\ h^{-1}\ cm^{-2}$ (-0.2 V vs. RHE) | 18.34 | Indophenol method | 15 |
| Ru SAs/N-C | 0.05 M $H_2SO_4$ | 120.9 $\mu g_{NH3}\ mg_{cat.}^{-1}\ h^{-1}$ (-0.1 V vs. RHE) | 30.84 $\mu g\ h^{-1}\ cm^{-2}$ (-0.1 V vs. RHE) | 29.6 | Indophenol method | 16 |
| $Fe_{SA}$-N-C | 0.1 M KOH | 7.48 $\mu g\ h^{-1}\ mg_{cat.}^{-1}$ (0.0 V vs. RHE) | 7.48 $\mu g\ h^{-1}\ cm^{-2}$ (0.0 V vs. RHE) | 56.55 | Indophenol method | 17 |
| SA-Mo/NPC | 0.1 M KOH | 34.0 ± 3.6 $\mu g_{NH3}\ h^{-1}\ mg_{cat.}^{-1}$ (-0.3 V vs. RHE) | 13.1 ± 1.4 $\mu g\ h^{-1}\ cm^{-2}$ (-0.3 V vs. RHE) | 14.6 ±1.6 | Nesslers method | 18 |
| Ru/$MoS_2$ | 10 mM HCl | $1.14 \times 10^{-10}$ mol $cm^{-2}\ s^{-1}$ (150 mV vs. RHE 50 ℃) | 6.98 $\mu g\ h^{-1}\ cm^{-2}$ (150 mV vs. RHE 50 ℃) | 17.6 | Indophenol method | 19 |
| $Pd_3Cu_1$ alloy | 1 M KOH | 39.9 mg $h^{-1}\ mg_{cat.}^{-1}$ (-0.25 V *vs.* RHE) | 15.96 $\mu g\ h^{-1}\ cm^{-2}$ (-0.25 V vs. RHE) | 1.56 (-0.05 V *vs.* RHE) | Nesslers method | 20 |
| $Mo_2C$ /C | 0.5 M $Li_2SO_4$ (pH=2) | 11.3 $\mu g\ h^{-1}\ mg_{Mo2C}^{-1}$ (-0.3 V vs. RHE) | / | 7.8 | Nesslers method | 21 |
| OVs-rich $MoO_2$ | 0.1 M HCl | 12.20 $\mu g\ h^{-1}\ mg_{cat.}^{-1}$ (-0.15 V vs. RHE) | 12.20 $\mu g\ h^{-1}\ cm^{-2}$ (-0.15 V vs. RHE) | 8.2 | Indophenol method | 22 |
| $TiO_2/Ti_3C_2Tx$ | 0.1 M HCl | 32.17 $\mu g\ h^{-1}\ mg_{cat.}^{-1}$ (-0.45 V *vs.* RHE) | 3.22 $\mu g\ h^{-1}\ cm^{-2}$ (-0.45 V vs. RHE) | 16.07 | Indophenol method | 23 |
| $Nb_2O_5$ nanofiber | 0.1 M HCl | 43.6 $\mu g\ h^{-1}\ mg_{cat.}^{-1}$. (-0.55 V vs. RHE) | / | 9.26 | Indophenol method | 24 |
| Fe/$Fe_3O_4$ | 0.1 M PBS (pH = 7.2) | ~0.19 $\mu g\ cm^{-2}\ h^{-1}$ (-0.3 V vs. RHE) | ~0.19 $\mu g\ h^{-1}\ cm^{-2}$ (-0.3 V vs. RHE) | 8.29 | Indophenol method | 25 |
| Fe-N/C-carbon nanotube | 0.1 M KOH | 34.83 $\mu g\ h^{-1}\ mg_{cat.}^{-1}$ (-0.2 V vs. RHE) | 17.42 $\mu g\ h^{-1}\ cm^{-2}$ (-0.2 V vs. RHE) | 9.28 | Indophenol method | 26 |
| MnO/TM | 0.1 M $Na_2SO_4$ | $1.11 \times 10^{-10}$ mol $s^{-1}\ cm^{-1}$ (-0.39 V vs. RHE) | 6.79 $\mu g\ h^{-1}\ cm^{-2}$ (-0.39 V vs. RHE) | 8.02 | Indophenol method | 27 |

| | | | | | | |
|---|---|---|---|---|---|---|
| Bismuth nanosheet (Bi NS) | 0.1 M $Na_2SO_4$ | 2.54 ± 0.16 $\mu g_{NH3}$ $cm^{-2}$ $h^{-1}$ ~13.23 μg $mg_{cat.}^{-1}$ $h^{-1}$ (-0.8 V *vs.* RHE) | 2.54 ± 0.16 μg $h^{-1}$ $cm^{-2}$ (-0.8 V vs. RHE) | 10.46 ± 1.45 | Indophenol method | 28 |
| BiNCs/CB/CP | 0.5 M $K_2SO_4$ (pH=3.5) | 200 mmol $g^{-1}$ $h^{-1}$ 0.052 mmol $cm^{-2}h^{-1}$ (-0.6 V vs. RHE) | 884 μg $h^{-1}$ $cm^{-2}$ (-0.6 V vs. RHE) | 66 | Nesslers method | 29 |
| ZIF-derived carbon | 0.1 M KOH | $3.4\times10^{-6}$ mol $cm^{-2}$ $h^{-1}$ (-0.3 V vs. RHE) | 57.8 μg $h^{-1}$ $cm^{-2}$ (-0.3 V vs. RHE) | 10.2 | Indophenol method | 30 |
| NPC-500 | 0.005 M $H_2SO_4$ | 1.31 mmol $g^{-1}$ $h^{-1}$ (-0.4 V vs. RHE) | 22.3 μg $h^{-1}$ $cm^{-2}$ (-0.4 V vs. RHE) | 9.98 | Indophenol method | 31 |
| $B_4C$ nanosheet | 0.1 M HCl | 26.57 μg $h^{-1}$ $mg_{cat.}^{-1}$ (-0.75 V *vs.* RHE) | 2.66 μg $h^{-1}$ $cm^{-2}$ (-0.75 V vs. RHE) | 15.95 | Indophenol method | 32 |
| Hollow $Cr_2O_3$ microspheres | 0.1 M $Na_2SO_4$ | 25.3 μg $h^{-1}$ $mg_{cat.}^{-1}$ (-0.55 V vs. RHE) | 3.04 μg $h^{-1}$ $cm^{-2}$ (-0.55 V vs. RHE) | 9.26 | Indophenol method | 33 |

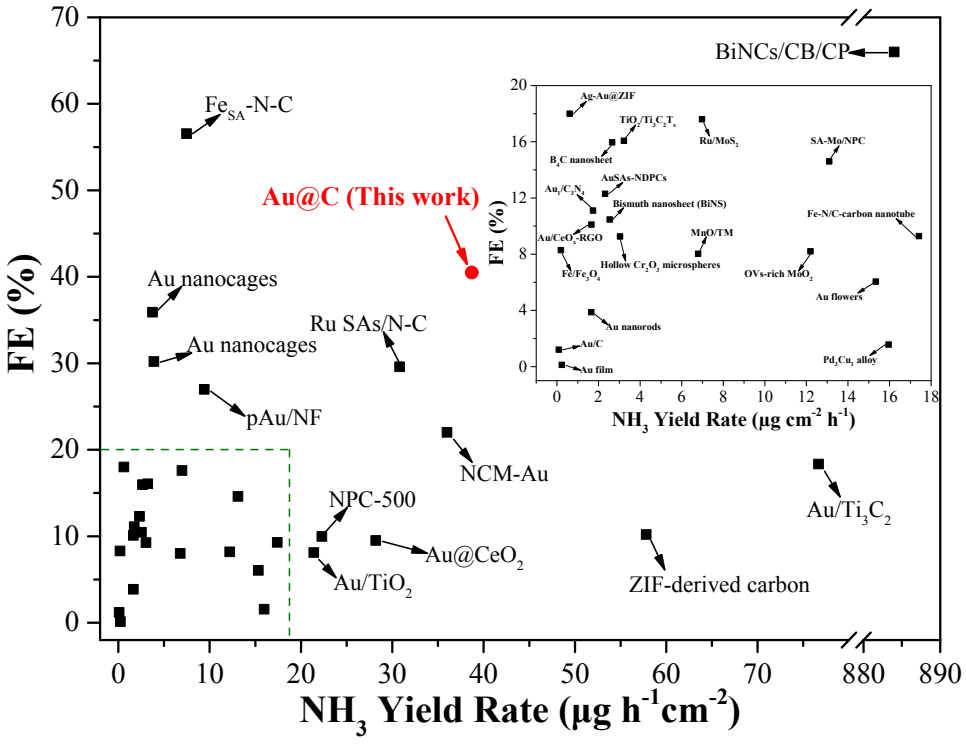


**Figure S1.** The $NH_3$ yield rate (μg $h^{-1}$ $cm^{-2}$) and FE (%) comparison of our work and other recently reported NRR electrocatalysts corresponding to Table S1.

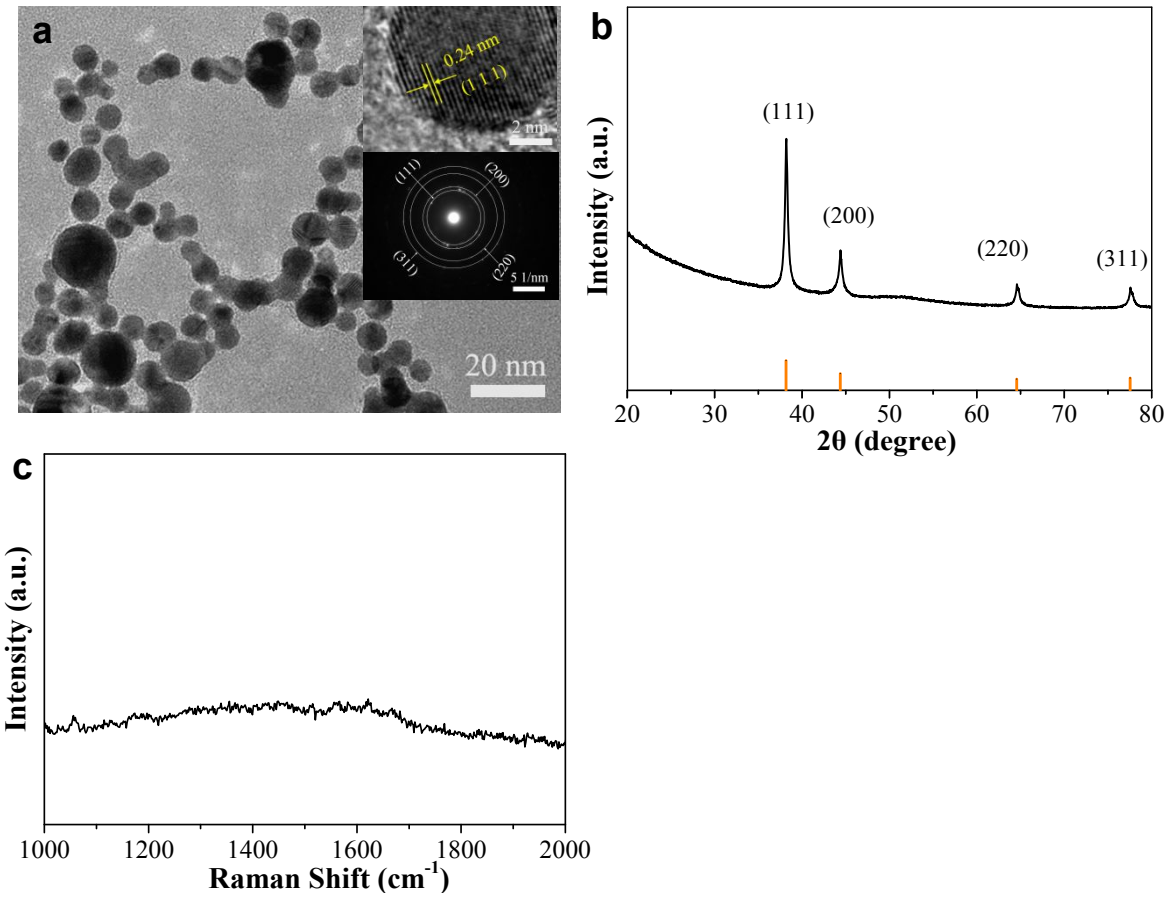


**Figure S2.** (a) TEM images and corresponding SAED patterns, (b) XRD patterns and (c) Raman spectrum of Au-NS sample.

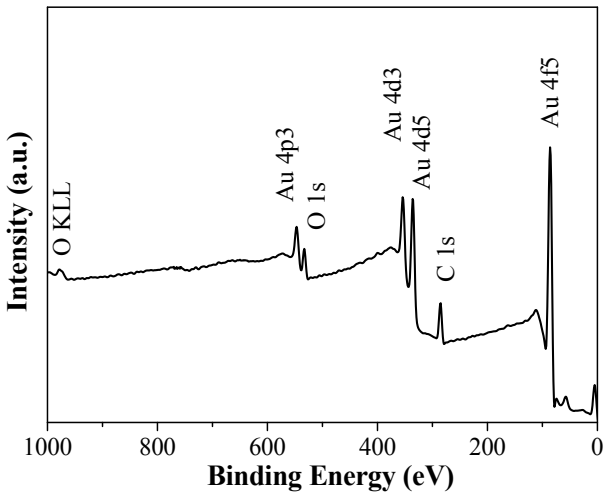


**Figure S3.** Surface survey XPS spectrum of Au@C sample.

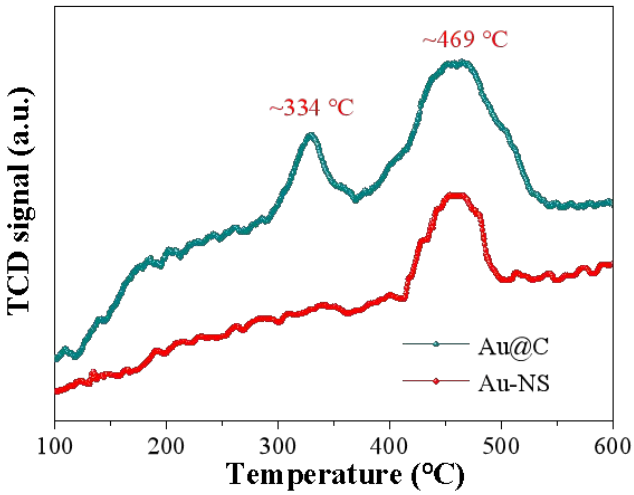


**Figure S4.** $N_2$ temperature programmed desorption ($N_2$-TPD) measurement curves of Au@C and Au-NS samples.

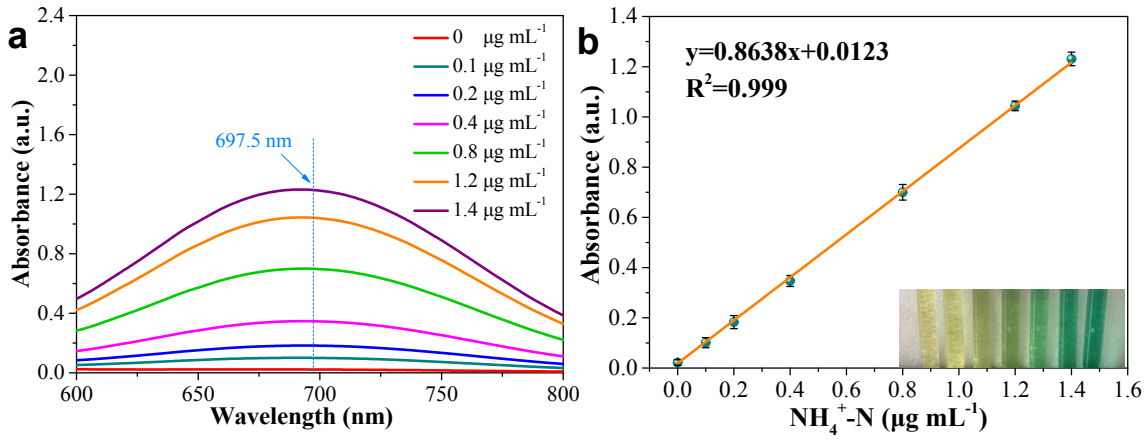


**Figure S5.** (a) UV-Vis absorbance spectra of the indophenol blue indicator with various concentrations of $NH_4^+$-N (0, 0.1, 0.2, 0.4, 0.8, 1.2, 1.4 μg $mL^{-1}$) after incubating for 1 h at room temperature. (b) The calibration curve used for calculation of $NH_4^+$-N concentration.

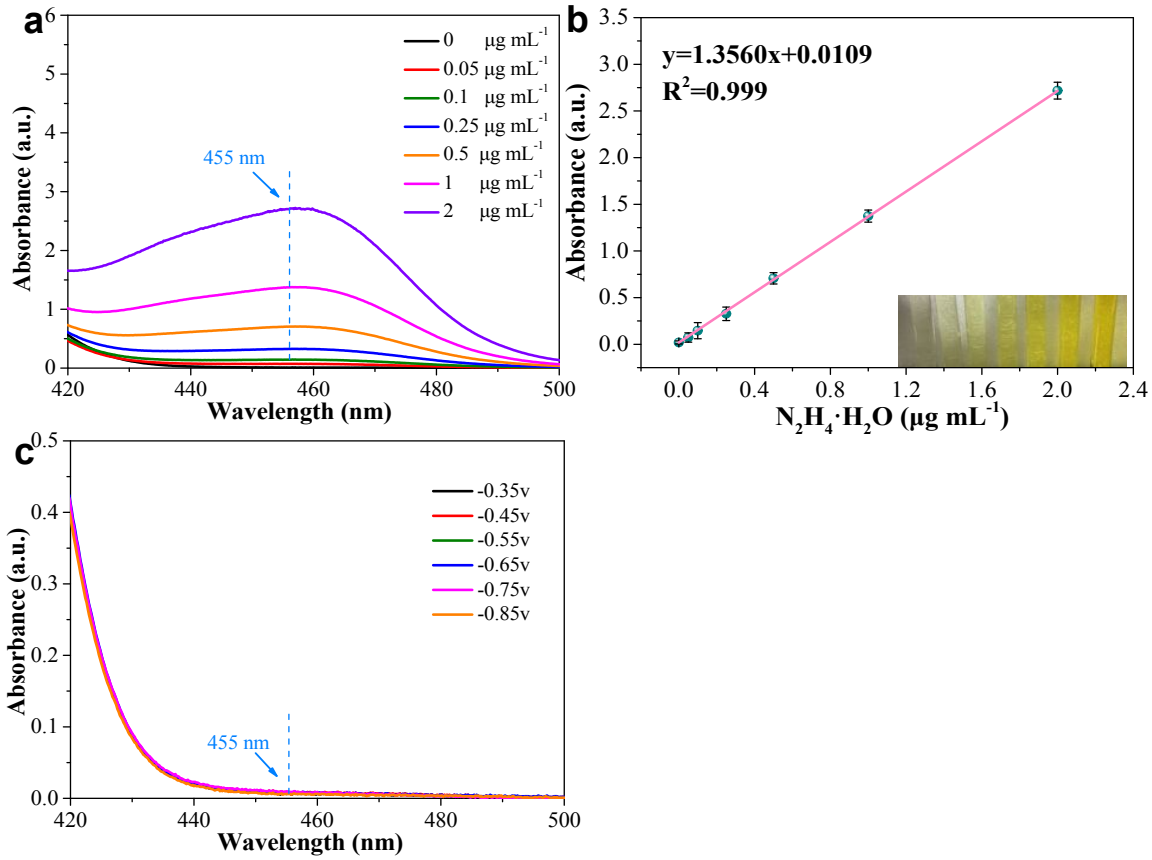


**Figure S6.** (a) UV-Vis absorption spectra with various concentrations of $N_2H_4 \cdot H_2O$ (0, 0.05, 0.1, 0.25, 0.5, 1.0, 2.0 μg $mL^{-1}$) after incubated for 20 min at room temperature. (b) The calibration curve used for calculation of $N_2H_4 \cdot H_2O$ concentrations. (c) UV-Vis absorption spectra of samples after NRR measurement at different potentials in 0.1 M $Na_2SO_4$ electrolyte.

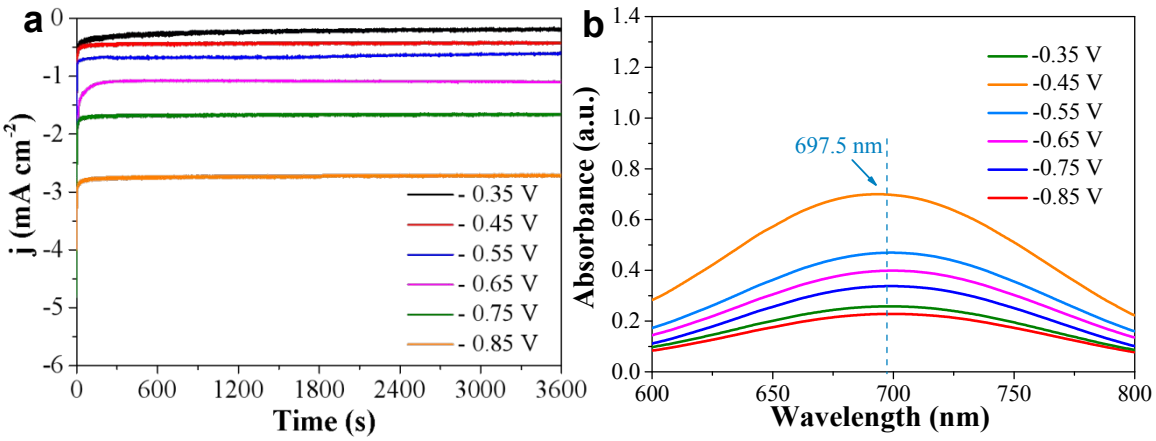


**Figure S7. (a)** Time-dependent current density curves of Au@C at different potentials in 0.1 M $Na_2SO_4$ electrolyte and (b) Corresponding UV-Vis absorption spectra of electrolytes colored with indophenols indicator after electrolysis at different potentials for 1 h.

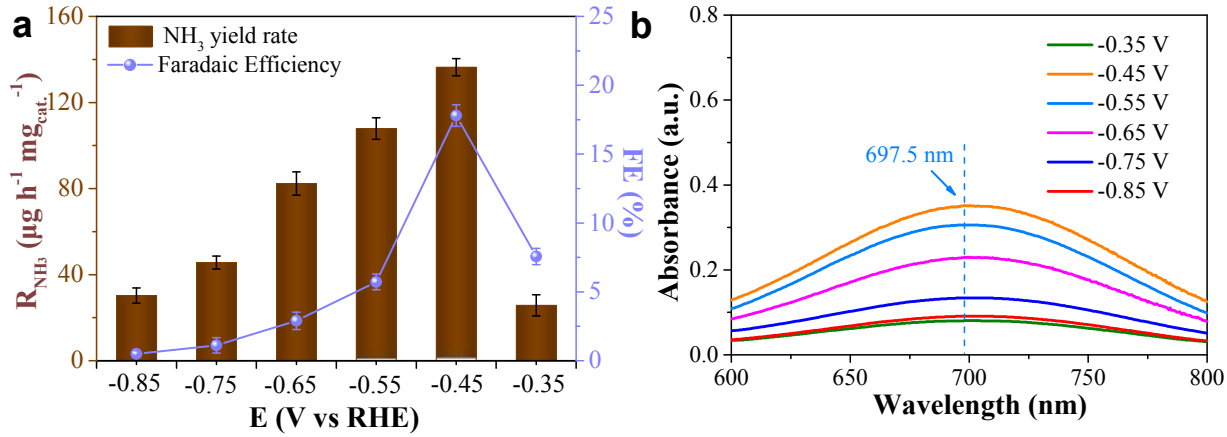


**Figure S8. (a)** The dependence of $NH_3$ yield rate and faradaic efficiency of Au-NS on applied potentials in $N_2$-saturated 0.1 M $Na_2SO_4$ electrolyte with NRR measurement time of 1 h. (b) Corresponding UV-Vis absorption spectra of electrolytes colored with indophenols indicator after electrolysis at different potentials for 1 h.

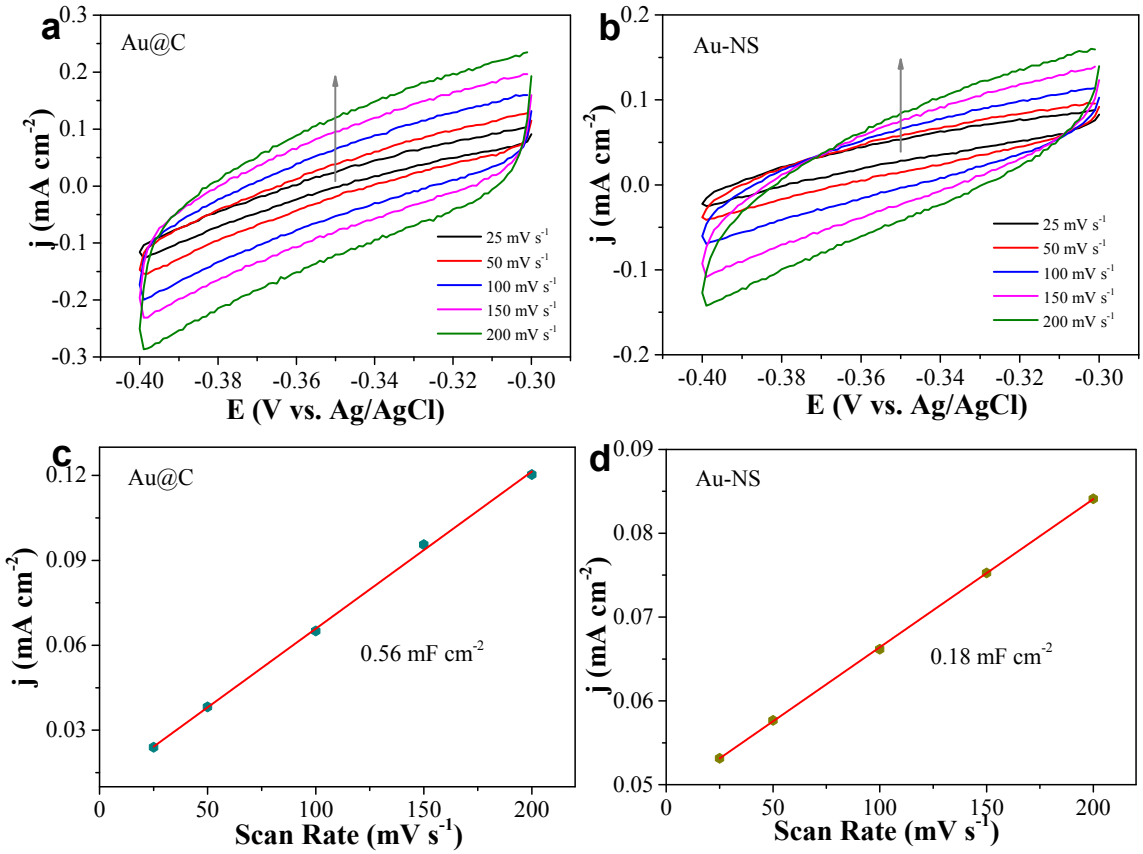


**Figure S9.** Cyclic voltammetry curves of (a) Au@C and (b) Au-NS with various scan rates (25, 50, 100, 150, 200 mV $s^{-1}$) in the region of –0.30 to –0.40 V *vs.* Ag/AgCl. The capacitive current densities at -0.35 V *vs.* Ag/AgCl as a function of scan rates for (c) Au@C and (d) Au-NS.

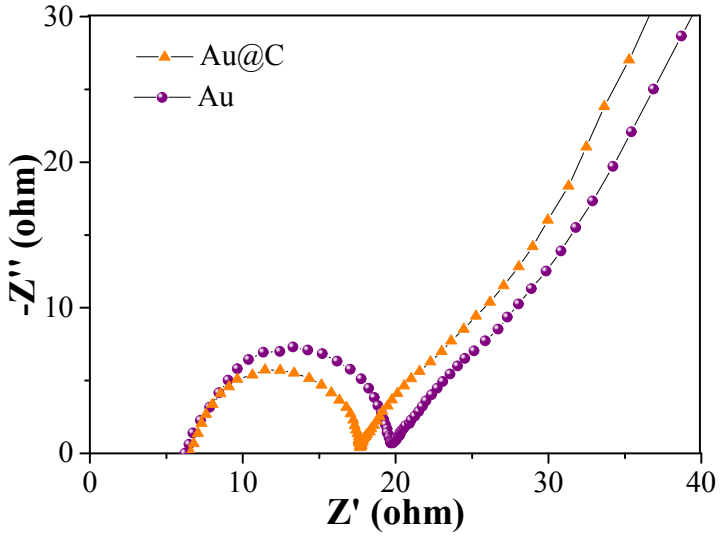


**Figure S10.** Electrochemical impedance spectra of Au@C and Au-NS obtained at -0.45 V (*vs.* RHE) in $N_2$-saturated 0.1 M $Na_2SO_4$ electrolyte.

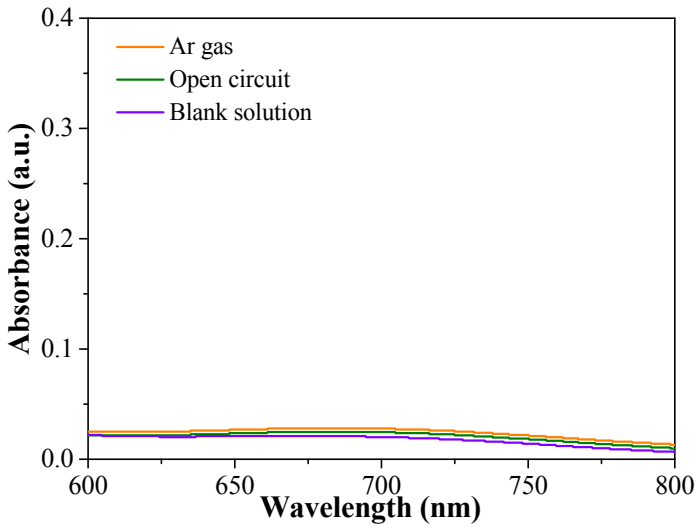


**Figure S11.** UV-Vis absorption spectra of blank solution ($N_2$-saturated 0.1 M $Na_2SO_4$ electrolyte), open-circuit condition (Au@C catalyst in $N_2$-saturated 0.1 M $Na_2SO_4$ electrolyte without applied potential for 1 h), and Ar-saturated electrolyte (Au@C catalyst in Ar-saturated 0.1 M $Na_2SO_4$ electrolyte with an applied potential of -0.45 V for 1 h). All solutions were incubated with indophenol indicator for 1 h before measurement.

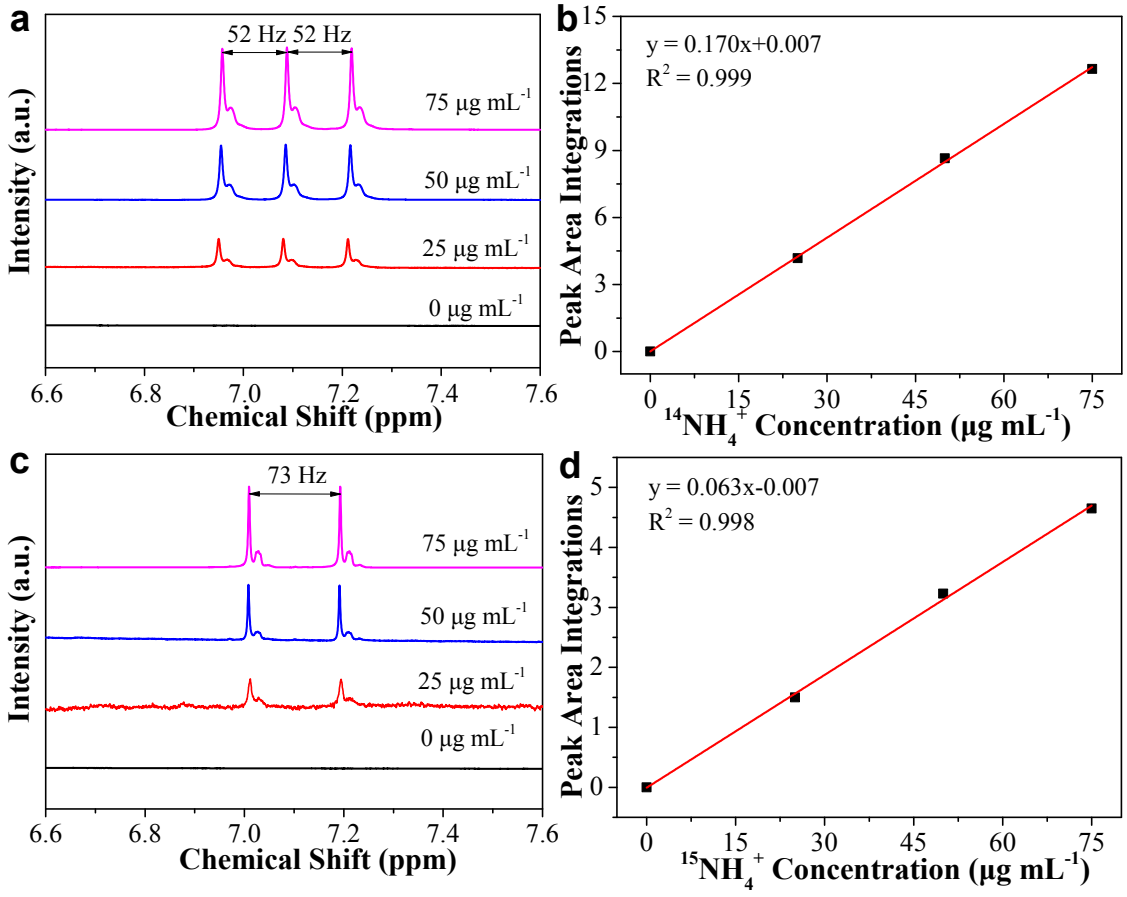


**Figure S12.** (a, c) $^{1}$H NMR spectra of the $^{14}NH_4^+$ and $^{15}NH_4^+$ concentrations; (b, d) Corresponding $^{14}NH_4^+$ and $^{15}NH_4^+$ calibration curves constructed by plotting the integrated $^{1}$H NMR peak area against standard concentration.

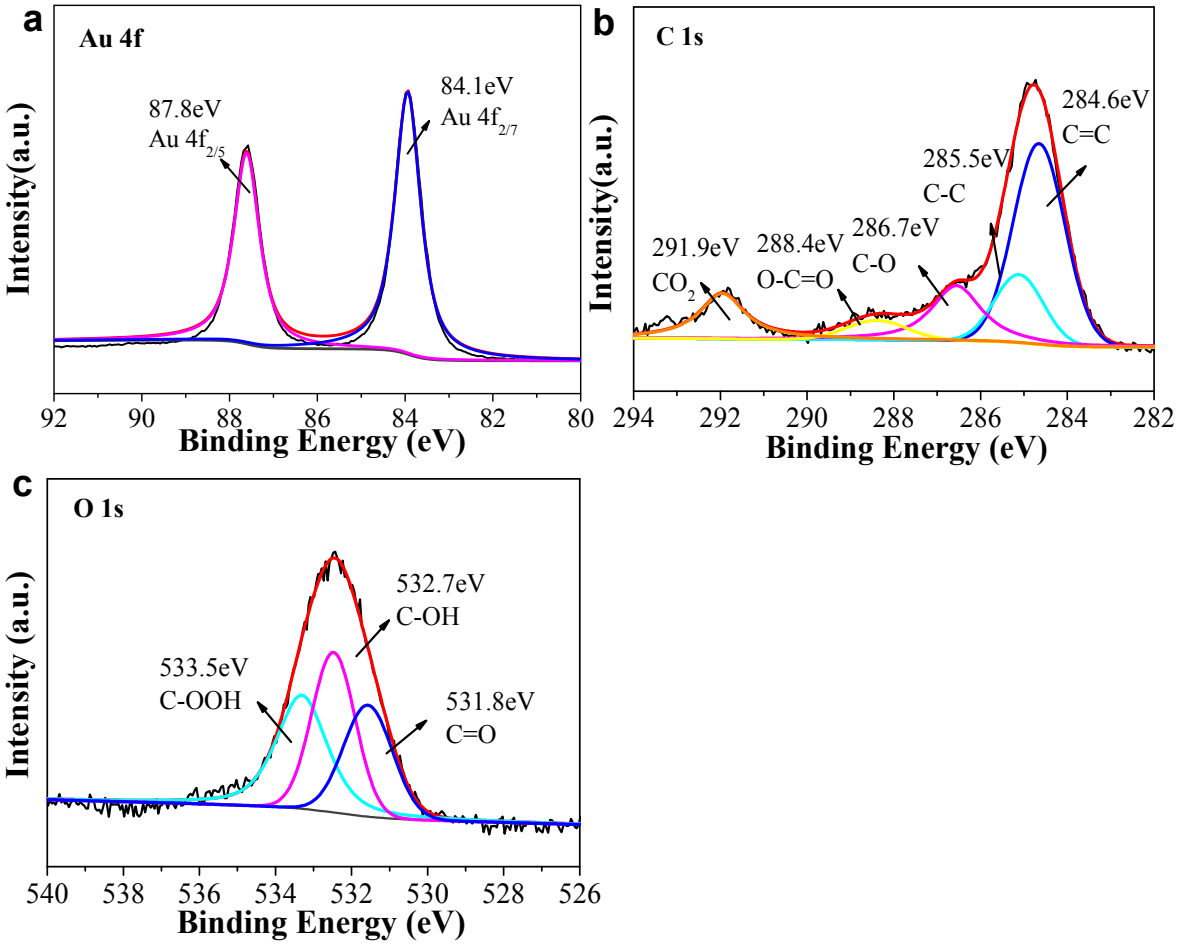


**Figure S13.** High resolution XPS spectra of Au 4f, C 1s and O 1s (a-c) of Au@C catalyst after 7 days NRR measurement at -0.45 V (vs. RHE) in $N_2$-saturated 0.1 M $Na_2SO_4$ electrolyte.

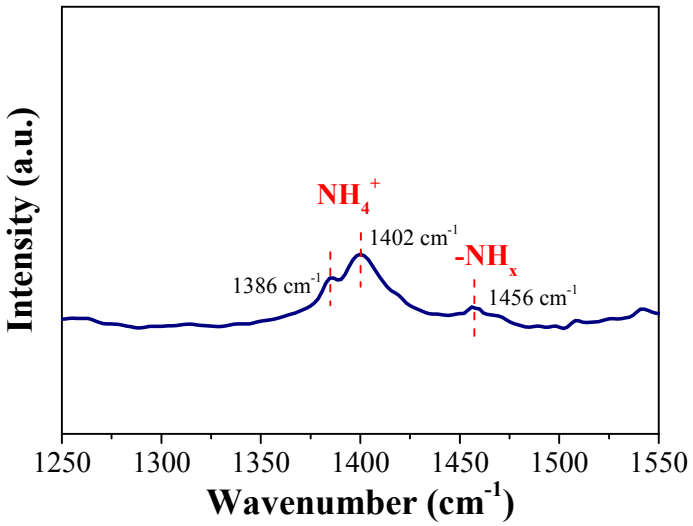


**Figure S14.** The FT-IR spectrum of the Au@C catalyst after 7 days NRR measurement at -0.45 V (vs. RHE) in $N_2$-saturated 0.1 M $Na_2SO_4$ electrolyte.

# References


(1) Shi, M. M.; Bao, D.; Wulan, B. R.; Li, Y. H.; Zhang, Y. F.; Yan, J. M.; Jiang, Q., Au Sub-Nanoclusters on $TiO_2$ toward Highly Efficient and Selective Electrocatalyst for $N_2$ Conversion to $NH_3$ at Ambient Conditions. *Adv. Mater.* **2017,** *29*, 1606550.

(2) Bao, D.; Zhang, Q.; Meng, F. L.; Zhong, H.X.; Shi, M. M.; Zhang, Y.; Yan, J. M.; Jiang, Q.; Zhang, X. B., Electrochemical Reduction of $N_2$ under Ambient Conditions for Artificial $N_2$ Fixation and Renewable Energy Storage Using $N_2/NH_3$ Cycle. *Adv. Mater.* **2017,** *29*, 1604799.

(3) Li, S. J.; Bao, D.; Shi, M. M.; Wulan, B. R.; Yan, J. M.; Jiang, Q., Amorphizing of Au Nanoparticles by $CeO_x$–RGO Hybrid Support towards Highly Efficient Electrocatalyst for $N_2$ Reduction under Ambient Conditions. *Adv. Mater.* **2017,** *29*, 1700001.

(4) Wang, J.; Yu, L.; Hu, L.; Chen, G.; Xin, H.; Feng, X., Ambient Ammonia Synthesis via Palladium-Catalyzed Electrohydrogenation of Dinitrogen at Low Overpotential. *Nat. Commun.* **2018,** *9*, 1795.

(5) Yao, Y.; Zhu, S.; Wang, H.; Li, H.; Shao, M., A Spectroscopic Study on the Nitrogen Electrochemical Reduction Reaction on Gold and Platinum Surfaces. *J. Am. Chem. Soc.* **2018,** *140*, 1496-1501.

(6) Wang, H.; Wang, L.; Wang, Q.; Ye, S.; Sun, W.; Shao, Y.; Jiang, Z.; Qiao, Q.; Zhu, Y.; Song, P.; Li, D.; He, L.; Zhang, X.; Yuan, J.; Wu, T.; Ozin, G. A., Ambient Electrosynthesis of Ammonia: Electrode Porosity and Composition Engineering. *Angew. Chem., Int. Ed.* **2018,** *57*, 12360-12364.

(7) Wang, Z.; Li, Y.; Yu, H.; Xu, Y.; Xue, H.; Li, X.; Wang, H.; Wang, L., Ambient Electrochemical Synthesis of Ammonia from Nitrogen and Water Catalyzed by Flower-Like Gold Microstructures. *ChemSusChem* **2018,** *11*, 3480-3485.

(8) Nazemi, M.; Panikkanvalappil, S. R.; El-Sayed, M. A., Enhancing the Rate of Electrochemical Nitrogen Reduction Reaction for Ammonia Synthesis under Ambient Conditions Using Hollow Gold Nanocages. *Nano Energy* **2018,** *49*, 316-323.

(9) Nazemi, M.; El-Sayed, M. A., Electrochemical Synthesis of Ammonia from $N_2$ and $H_2O$ under Ambient Conditions Using Pore-Size-Controlled Hollow Gold Nanocatalysts with Tunable Plasmonic Properties. *J. Phys. Chem. Lett.* **2018,** *9*, 5160-5166.

(10) Qin, Q.; Heil, T.; Antonietti, M.; Oschatz, M., Single-Site Gold Catalysts on Hierarchical N-Doped Porous Noble Carbon for Enhanced Electrochemical Reduction of Nitrogen. *Small Methods* **2018,** *2*, 1800202.

(11) Lee, H. K.; Koh, C. S.; Lee, Y. H.; Liu, C.; Phang, I. Y.; Han, X.; Tsung, C. K.; Ling, X. Y., Favoring the Unfavored: Selective Electrochemical Nitrogen Fixation Using a Reticular Chemistry Approach. *Sci. Adv.* **2018,** *4*, eaar3208.

(12) Wang, X.; Wang, W.; Qiao, M.; Wu, G.; Chen, W.; Yuan, T.; Xu, Q.; Chen, M.; Zhang, Y.; Wang, X.; Wang, J.; Ge, J.; Hong, X.; Li, Y.; Wu, Y.; Li, Y., Atomically

Dispersed $Au_1$ Catalyst towards Efficient Electrochemical Synthesis of Ammonia. *Sci. Bull.* **2018,** *63*, 1246-1253.

(13) Wang, H.; Yu, H.; Wang, Z.; Li, Y.; Xu, Y.; Li, X.; Xue, H.; Wang, L., Electrochemical Fabrication of Porous Au Film on Ni Foam for Nitrogen Reduction to Ammonia. *Small Methods* **2019,** *15*, 1804769.

(14) Zhang, H.; Liu, G.; Cui, Z.; Han, M.; Zhang, S.; Zhao, C.; Chen, C.; Wang, G., Ambient Electrosynthesis of Ammonia on Core-Shell Structure Au@$CeO_2$ Catalyst: Contribution of Oxygen Vacancies in $CeO_2$. *Chem. Eur. J.* **2019,** *25,* 5904-5911.

(15) Liu, D.; Zhang, G.; Ji, Q.; Zhang, Y.; Li, J., Synergistic Electrocatalytic Nitrogen Reduction Enabled by Confinement of Nanosized Au Particles onto a Two-Dimensional $Ti_3C_2$ Substrate. *ACS Appl. Mater. Interfaces* **2019,** *11*, 25758-25765.

(16) Geng, Z.; Liu, Y.; Kong, X.; Li, P.; Li, K.; Liu, Z.; Du, J.; Shu, M.; Si, R.; Zeng, J., Achieving a Record-High Yield Rate of 120.9 $\mu g_{NH3}$ $mg_{cat.}^{-1}$ $h^{-1}$ for $N_2$ Electrochemical Reduction over Ru Single-Atom Catalysts. *Adv. Mater.* **2018,** *30*, 1803498.

(17) Wang, M.; Liu, S.; Qian, T.; Liu, J.; Zhou, J.; Ji, H.; Xiong, J.; Zhong, J.; Yan, C., Over 56.55% Faradaic Efficiency of Ambient Ammonia Synthesis Enabled by Positively Shifting the Reaction Potential. *Nat. Commun.* **2019,** *10*, 341.

(18) Han, L.; Liu, X.; Chen, J.; Lin, R.; Liu, H.; Lu, F.; Bak, S.; Liang, Z.; Zhao, S.; Stavitski, E.; Luo, J.; Adzic, R. R.; Xin, H. L., Atomically Dispersed Molybdenum Catalysts for Efficient Ambient Nitrogen Fixation. *Angew. Chem., Int. Ed.* **2019,** *58*, 2321-2325.

(19) Suryanto, B. H.; Wang, D.; Azofra, L. M.; Harb, M.; Cavallo, L.; Jalili, R.; Mitchell, D. R. G.; Chatti, M.; MacFarlane, D. R., $MoS_2$ Polymorphic Engineering Enhances Selectivity in the Electrochemical Reduction of Nitrogen to Ammonia. *ACS Energy Lett.* **2019,** *4*, 430-435.

(20) Pang, F.; Wang, Z.; Zhang, K.; He, J.; Zhang, W.; Guo, C.; Ding, Y., Bimodal Nanoporous $Pd_3Cu_1$ Alloy with Restrained Hydrogen Evolution for Stable and High Yield Electrochemical Nitrogen Reduction. *Nano Energy* **2019,** *58*, 834-841.

(21) Cheng, H.; Ding, L. X.; Chen, G. F.; Zhang, L.; Xue, J.; Wang, H., Molybdenum Carbide Nanodots Enable Efficient Electrocatalytic Nitrogen Fixation under Ambient Conditions. *Adv. Mater.* **2018,** *30*, 1803694.

(22) Zhang, G.; Ji, Q.; Zhang, K.; Chen, Y.; Li, Z.; Liu, H.; Li, J.; Qu, J., Triggering Surface Oxygen Vacancies on Atomic Layered Molybdenum Dioxide for a Low Energy Consumption Path toward Nitrogen Fixation. *Nano Energy* **2019,** *59*, 10-16.

(23) Fang, Y.; Liu, Z.; Han, J.; Jin, Z.; Han, Y.; Wang, F.; Niu, Y.; Wu, Y.; Xu, Y., High-Performance Electrocatalytic Conversion of $N_2$ to $NH_3$ Using Oxygen-Vacancy-Rich $TiO_2$ In Situ Grown on $Ti_3C_2T_x$ MXene. *Adv. Energy Mater.* **2019,** *0*, 1803406.

(24) Han, J.; Liu, Z.; Ma, Y.; Cui, G.; Xie, F.; Wang, F.; Wu, Y.; Gao, S.; Xu, Y.; Sun, X., Ambient $N_2$ Fixation to $NH_3$ at Ambient Conditions: Using $Nb_2O_5$ Nanofiber as a High-Performance Electrocatalyst. *Nano Energy* **2018,** *52*, 264-270.

(25) Hu, L.; Khaniya, A.; Wang, J.; Chen, G.; Kaden, W. E.; Feng, X., Ambient Electrochemical Ammonia Synthesis with High Selectivity on Fe/Fe Oxide Catalyst. *ACS Catal.* **2018,** *8*, 9312-9319.

(26) Wang, Y.; Cui, X.; Zhao, J.; Jia, G.; Gu, L.; Zhang, Q.; Meng, L.; Shi, Z.; Zheng, L.; Wang, C.; Zhang, Z.; Zheng, W., Rational Design of Fe–N/C Hybrid for Enhanced Nitrogen Reduction Electrocatalysis under Ambient Conditions in Aqueous Solution. *ACS Catal.* **2019,** *9*, 336-344.

(27) Wang, Z.; Gong, F.; Zhang, L.; Wang, R.; Ji, L.; Liu, Q.; Luo, Y.; Guo, H.; Li, Y.; Gao, P.; Shi, X.; Li, B.; Tang, B.; Sun, X., Electrocatalytic Hydrogenation of $N_2$ to $NH_3$ by MnO: Experimental and Theoretical Investigations. *Adv. Sci.* **2019,** *6*, 1801182.

(28) Li, L.; Tang, C.; Xia, B.; Jin, H.; Zheng, Y.; Qiao, S. Z., Two-Dimensional Mosaic Bismuth Nanosheets for Highly Selective Ambient Electrocatalytic Nitrogen Reduction. *ACS Catal.* **2019**, *9*, 2902-2908.

(29) Hao, Y. C.; Guo, Y.; Chen, L. W.; Shu, M.; Wang, X. Y.; Bu, T. A.; Gao, W. Y.; Zhang, N.; Su, X.; Feng, X.; Zhou, J. W.; Wang, B.; Hu, C. W.; Yin, A. X.; Si, R.; Zhang, Y. W.; Yan, C. H., Promoting Nitrogen Electroreduction to Ammonia with Bismuth Nanocrystals and Potassium Cations in Water. *Nat. Catal.* **2019**, *2*, 448-456.

(30) Mukherjee, S.; Cullen, D. A.; Karakalos, S.; Liu, K.; Zhang, H.; Zhao, S.; Xu, H.; More, K. L.; Wang, G.; Wu, G., Metal-Organic Framework-Derived Nitrogen-Doped Highly Disordered Carbon for Electrochemical Ammonia Synthesis Using $N_2$ and $H_2O$ in Alkaline Electrolytes. *Nano Energy* **2018,** *48*, 217-226.

(31) Zhao, C.; Zhang, S.; Han, M.; Zhang, X.; Liu, Y.; Li, W.; Chen, C.; Wang, G.; Zhang, H.; Zhao, H., Ambient Electrosynthesis of Ammonia on a Biomass-Derived Nitrogen-Doped Porous Carbon Electrocatalyst: Contribution of Pyridinic Nitrogen. *ACS Energy Lett.* **2019**, *4*, 377-383.

(32) Qiu, W.; Xie, X. Y.; Qiu, J.; Fang, W. H.; Liang, R.; Ren, X.; Ji, X.; Cui, G.; Asiri, A. M.; Cui, G.; Tang, B.; Sun, X., High-Performance Artificial Nitrogen Fixation at Ambient Conditions Using a Metal-Free Electrocatalyst. *Nat. Commun.* **2018,** *9*, 3485.

(33) Zhang, Y.; Qiu, W.; Ma, Y.; Luo, Y.; Tian, Z.; Cui, G.; Xie, F.; Chen, L.; Li, T.; Sun, X., High-Performance Electrohydrogenation of $N_2$ to $NH_3$ Catalyzed by Multishelled Hollow $Cr_2O_3$ Microspheres under Ambient Conditions. *ACS Catal.* **2018,** *8*, 8540-8544.